Heat Capacity of the Spin Crossover Complex $[Fe(2\text{-pic})_3]Cl_2\cdot MeOH$: A Spin Crossover Phenomenon with Weak Cooperativity in the Solid State[†]

Tadahiro Nakamoto,[‡] Zhi-Cheng Tan,[‡,§] and Michio Sorai*,[‡]

Research Center for Molecular Thermodynamics, Graduate School of Science, Osaka University,
Toyonaka, Osaka 560-0043, Japan, and Thermochemistry Laboratory, Dalian Institute of Chemical
Physics, Chinese Academy of Sciences, Dalian 116023, China

Received January 18, 2001

Heat capacities of the spin crossover complex $[Fe(2\text{-pic})_3]Cl_2\cdot MeOH$ (2-pic: 2-picolylamine or 2-aminomethylpyridine) were measured with an adiabatic calorimeter between 12 and 355 K. A broad heat capacity peak, starting from ∼80 K, culminating at ∼150 K, and terminating at ∼250 K, was observed. The temperature range of the heat capacity anomaly corresponds to that where the low-spin and high-spin states coexist in the ^{57}Fe Mössbauer spectra. The enthalpy and entropy changes arising from the heat capacity anomaly were 8.88 kJ mol^{-1} and 59.5 J K^{-1} mol^{-1}, respectively. The entropy gain was much larger than the contribution expected from the change in the spin-manifold $R \ln 5$ (13.4 J K^{-1} mol^{-1}) where R is the gas constant. The remaining entropy gain is attributed to the contribution from the change in the internal vibrations. On the basis of the domain model, the number of molecules per domain was found to be very close to unity, implying a very weak cooperativity in the spin crossover occurring in the solid state of this complex.

Introduction

Complexes whose ligand fields are located near the high-spin (HS) and the low-spin (LS) crossover region have been known to show a temperature-induced spin crossover phenomenon. The characteristics of this phenomenon have been understood by many experimental and theoretical approaches.[1−3] The spin crossover system most extensively investigated is octahedral ferrous (Fe^{II}) complexes which undergo the spin transition between LS ($^1A_{1g}$, $S = 0$) at low temperatures and HS ($^5T_{2g}$, $S = 2$) at high temperatures, where S stands for the spin quantum number. As widely recognized, the temperature-induced spin crossover phenomena are classified into two groups; one is the so-called "abrupt type" in which the spin state conversion between the LS and the HS states takes place within a narrow temperature range ($<\sim 10$ K) and often accompanied by a hysteresis, while the other is the so-called "gradual type" in which the spin-state conversion takes place over a wider temperature range than ∼100 K. In the case of the abrupt-type compounds, a sharp phase transition is observed in heat capacity measurements at the temperature corresponding to the abrupt spin transition. Sorai and Seki[4] observed, for the first time, a sharp heat capacity peak in two spin transition type complexes, $[Fe(phen)_2(NCS)_2]$ at 176.29 K and $[Fe(phen)_2(NCSe)_2]$ at 231.26 K, where phen = 1,10-phenanthroline, and suggested the spin transitions are cooperative phenomena proceeding via significant coupling between the electronic state and the phonon system. They have proposed the domain model for a better understanding of the spin crossover behavior. The model well accounts for the nature of the "cooperativity" of the continuous type spin crossover phenomena in terms of the number of molecules per domain n. It is comprehensible that the larger the value of n, the higher the cooperativity is, while the cooperativity in spin crossover phenomena becomes lower as the n approaches unity. According to the domain model, n was estimated to be 95 for $[Fe(phen)_2(NCS)_2]$ and 77 for $[Fe(phen)_2(NCSe)_2]$.

In the case of the gradual type spin crossover complexes, because of the low cooperativity in spin crossover phenomenon, they exhibit no sharp heat capacity peak as exemplified by ferric (Fe^{III}) spin crossover complexes.[5−9] However, the spin crossover complex $[Fe(2\text{-pic})_3]Cl_2\cdot EtOH$, which seems to belong to the gradual type, exhibits well-resolved double peaks in the heat capacity arising from the phase transitions as well as a broad heat capacity hump extending over a wide temperature range.[10,11] Since an order−disorder transition concerning the ethanol solvate molecule was found by the multi-temperature single-crystal X-ray structure determination,[12] the cooperative nature of the spin crossover in this compound was explained in terms

---

* To whom correspondence should be addressed. Tel: +81-6-6850-5523. Fax: +81-6-6850-5526. E-mail: sorai@chem.sci.osaka-u.ac.jp.

[†] Contribution No. 42 from the Research Center for Molecular Thermodynamics.

[‡] Osaka University.

[§] Chinese Academy of Sciences.

(1) König, E. *Prog. Inorg. Chem.* **1987**, *35*, 527; *Struct. Bonding* **1991**, *76*, 51.
(2) Gütlich, P.; Hauser, A.; Spiering, H. *Angew. Chem., Int. Ed. Engl.* **1994**, *33*, 2024.
(3) Kahn, O.; Kröber, J.; Jay, C. *Adv. Mater.* **1992**, *4*, 718.
(4) Sorai, M.; Seki, S. *J. Phys. Chem. Solids* **1974**, *35*, 555.
(5) Sorai, M.; Maeda, Y.; Oshio, H. *J. Phys. Chem. Solids* **1990**, *51*, 941.
(6) Conti, A. J.; Kaji, K.; Nagano, Y.; Sena, K. M.; Yumoto, Y.; Chadha, R. K.; Rheingold, A. L.; Sorai, M.; Hendrickson, D. N. *Inorg. Chem.* **1993**, *32*, 2681.
(7) Kaji, K.; Sorai, M.; Conti, A. J.; Hendrickson, D. N. *J. Phys. Chem. Solids* **1993**, *54*, 1621.
(8) Sorai, M.; Nagano, Y.; Conti, A. J.; Hendrickson, D. N. *J. Phys. Chem. Solids* **1994**, *55*, 317.
(9) Sorai, M.; Yumoto, Y.; Hendrickson, D. N. 42nd Annual Meeting on Coordination Chemistry, Nara, 3B08, 1992.
(10) Kaji, K.; Sorai, M. *Thermochim. Acta* **1985**, *88*, 185.
(11) Jakobi, R.; Spiering, H.; Gütlich, P. *J. Phys. Chem Solids* **1992**, *53*, 267.
(12) Mikami, M.; Konno, M.; Saito, Y. *Chem. Phys. Lett.* **1979**, *63*, 566; *Acta Crystallogr.* **1980**, *B36*, 275.

10.1021/ic010073z CCC: $20.00

of strong coupling between the reorientational motions of ethanol solvate molecule and the spin crossover. Evidence for domains in the spin crossover phenomenon of $[Fe(2\text{-pic})_3]Cl_2\cdot EtOH$ has been found by means of EPR.[13] Calorimetric measurements so far made for the gradual type complexes involving no reorientational disorder of solvate molecule or counteranion are $[Fe^{III}(acpa)_2]PF_6$ (Hacpa = *N*-(1-acetyl-2-propylidene)(2-pyridylmethyl)amine)[5] and $[Fe^{III}(3\text{-OEt-SalAPA})_2]ClO_4\cdot S$ (S = C_6H_5Br or *o*-$C_6H_4Cl_2$), where 3-OEt-SalAPA$^-$ is the monoanion of the Schiff base condensate of 3-ethoxysalicylaldehyde and *N*-(3-aminopropyl)aziridine.[6,9] These complexes exhibited only a broad heat capacity hump over a wide temperature range corresponding to the spin crossover phenomenon. According to the domain model, the number of complexes per domain was estimated to be $n = 5$ for $[Fe^{III}(acpa)_2]PF_6$,[5] indicating that there remains some cooperativity in the spin crossover phenomenon of this complex, although the cooperativity is weak. In the case of $[Fe^{III}(3\text{-OEt-SalAPA})_2]ClO_4\cdot S$ (S = C_6H_5Br or *o*-$C_6H_4Cl_2$), the broad heat capacity anomalies were well reproduced by the van't Hoff equation, implying that the spin crossover in these complexes proceeds in an equilibrium fashion between two-energy-level scheme.[6,9]

The present iron(II) complex $[Fe(2\text{-pic})_3]Cl_2\cdot MeOH$ is classified into the gradual transition type because the spin transition occurs over a wide temperature range from ~100 to ~250 K. Close investigations by variable temperature X-ray structure determination[14] and Mössbauer measurements[15] indicated that the spin transition in this compound is essentially noncooperative. This complex is, therefore, considered to be suitable for the elucidation of the intrinsic thermal properties characteristic of the noncooperative spin crossover phenomenon. Since no calorimetric study has been ever performed for this complex, we measured its heat capacities and identified the noncooperativity of the spin crossover phenomenon.

Experimental Section

Compound Preparation. The sample was prepared by the method previously reported[15] with slight modifications.

$[Fe(2\text{-pic})_3]Cl_2\cdot 2H_2O$. To a concentrated Fe^{3+}-free aqueous solution of $FeCl_2\cdot 4H_2O$ was added 3 equiv of 2-aminomethylpyridine (2-picolylamine). Dark red crystals formed after slow evaporation under nitrogen stream were filtered off, washed with 2-butoxyethanol and acetone, and then dried under nitrogen stream. Anal. Calcd for $C_{18}H_{28}N_6O_2FeCl_2$: C, 44.37; H, 5.79; N, 17.24. Found: C, 44.47; H, 5.81; N, 17.45.

$[Fe(2\text{-pic})_3]Cl_2\cdot H_2O$. The monohydrate was prepared by partial dehydration of the dihydrate under helium stream at 60−70 °C in a water bath until the dark red crystals completely turned into a yellow powder. This compound easily absorbs moisture when it is exposed to air as evidenced by the immediate color change to red. Anal. Calcd for $C_{18}H_{26}N_6OFeCl_2$: C, 46.07; H, 5.58; N, 17.91. Found: C, 46.22; H, 5.60; N, 17.95.

$[Fe(2\text{-pic})_3]Cl_2\cdot MeOH$. The methanol-solvated compound was prepared by recrystalization of the monohydrate from methanol under nitrogen. The yellow crystals were filtered off and dried under nitrogen stream. Anal. Calcd for $C_{19}H_{28}N_6OFeCl_2$: C, 47.23; H, 5.84; N, 17.39. Found: C, 46.98; H, 5.90; N, 17.31.

Heat Capacity Measurements. Heat capacity measurements between 13 and 355 K were made with a home-built adiabatic calorimeter.[16] The mass of sample used for the calorimetry was 6.40883 g (13.2628 mmol). A small amount of He gas was sealed in the calorimeter cell to aid the heat transfer.

Results and Discussion

The molar heat capacities under constant pressure, C_p, of $[Fe(2\text{-pic})_3]Cl_2\cdot MeOH$ at temperatures between 12 and 355 K are plotted in Figure 1 and listed in Table 1. A broad heat capacity anomaly, starting from ~80 K, culminating at ~150 K, and terminating at ~250 K, was observed. The starting temperature just corresponds to that where the quadrupole-split doublet due to the HS component appears in the ^{57}Fe Mössbauer spectrum, and the terminating temperature corresponds to the temperature where the LS component disappears from the ^{57}Fe Mössbauer spectrum. The culminating temperature roughly corresponds to the temperature at which the HS and the LS fractions, as measured by ^{57}Fe Mössbauer spectrum, are equal. Therefore, the heat capacity hump obviously arises from the spin crossover phenomenon.

For determination of the excess heat capacities due to the spin crossover phenomenon, it is necessary to estimate a normal heat capacity curve or lattice heat capacity, C_{lat}. The normal heat capacity curve was determined by the same manner as described previously.[5] The normal heat capacity curves of the LS state $C_{lat}(LS)$ and the HS state $C_{lat}(HS)$ were independently determined by the effective frequency distribution method.[17] For determination of the $C_{lat}(LS)$, we used 45 C_p values in the 12−80 K temperature range. On the other hand, for the estimate of $C_{lat}(HS)$, 40 C_p values in the 250−355 K and 10 C_p values in the 12−23 K temperature range were used. These 10 low-temperature C_p values were considered to correspond to the values for the HS state. Without this treatment, the effective frequency distribution method brought about trivial results owing to the lack of data over a wide temperature interval from 0 to 250 K. The "best" $C_{lat}(LS)$ and $C_{lat}(HS)$ curves determined by the least-squares fitting are reproduced in Figure 1. The normal heat capacity curve, C_{lat}, was finally evaluated by the following equation

$$C_{lat} = f_{HS}C_{lat}(HS) + (1 - f_{HS})C_{lat}\,(LS) \qquad (1)$$

Here, f_{HS} is the HS fraction determined by the equation

$$f_{HS} = \frac{1}{1 + \exp\left(\frac{\Delta G}{RT}\right)} \qquad (2)$$

and

$$\frac{\Delta G}{R} = -0.006713T^2 - 5.969T + 1072 \qquad (3)$$

where T stands for temperature, R is the gas constant, and ΔG corresponds to the Gibbs energy difference between the HS and the LS states. Equations 2 and 3 were determined by the least-squares fit of the HS area fraction of ^{57}Fe Mössbauer spectra vs temperature taken from the previous report.[15] The difference between the observed and the normal heat capacities shown in Figure 2 corresponds to the excess heat capacity, ΔC_p, due to the spin crossover phenomenon. The excess enthalpy, $\Delta_{trs}H$, and entropy, $\Delta_{trs}S$, arising from the spin crossover phenomenon were determined by integration of ΔC_p with respect to T and ln T, respectively. The total enthalpy and entropy gains are $\Delta_{trs}H = 8.88$ kJ mol^{-1} and $\Delta_{trs}S = 59.5$ J K^{-1} mol^{-1}, respectively.

---

(13) Doan, P. E.; McGarvey, B. R. *Inorg. Chem.* **1990**, *29*, 874.
(14) Katz, B. A.; Strouse, C. E. *J. Am. Chem. Soc.* **1979**, *101*, 6214.
(15) Sorai, M.; Ensling, J.; Hasselbach, K. M.; Gütlich, P. *Chem. Phys.* **1977**, *20*, 197.
(16) Sorai, M.; Nishimori, A.; Nagano, Y. Unpublished results.
(17) Sorai, M.; Seki, S. *J. Phys. Soc. Jpn.* **1972**, *32*, 382.

Table 1. Molar Heat Capacities of the Spin Crossover Complex [Fe(2-pic)$_3$]Cl$_2$·MeOH (Relative Molar Mass 483.22)

T (K)	C_p (J K^{-1} mol^{-1})	T (K)	C_p (J K^{-1} mol^{-1})	T (K)	C_p (J K^{-1} mol^{-1})
12.293	16.49	93.237	225.16	219.613	438.15
13.288	19.90	95.516	230.46	222.290	441.49
14.477	23.72	97.849	236.33	225.038	444.72
15.686	27.53	100.236	242.43	227.775	447.92
16.918	31.38	102.572	248.77	230.500	451.09
18.154	35.24	104.861	255.66	233.210	454.58
19.397	39.11	107.105	262.78	235.911	458.16
20.645	43.23	109.502	271.11	238.599	462.04
21.967	47.56	112.045	280.92	241.276	465.74
23.336	52.02	114.533	291.51	243.941	468.88
24.685	56.52	116.966	302.99	246.595	472.91
26.090	61.10	119.346	315.35	249.238	476.67
27.585	65.84	121.674	328.48	251.870	480.19
29.152	70.91	123.950	342.98	254.492	484.28
30.683	75.59	126.451	360.27	257.103	488.00
31.411	77.98	129.164	380.90	259.702	491.71
33.066	83.13	131.895	402.01	262.291	495.66
34.890	88.69	134.558	421.01	264.870	499.48
36.557	93.45	136.408	432.78	267.438	503.63
38.098	98.19	137.564	439.69	269.997	507.04
39.537	102.28	138.711	445.15	272.545	510.67
40.895	106.09	139.849	450.77	275.084	514.35
42.182	109.59	141.542	456.78	277.612	518.66
43.408	113.06	143.464	462.04	280.131	522.16
44.580	116.31	145.371	465.49	282.641	526.51
45.703	119.54	147.264	468.10	285.140	530.55
46.786	122.38	149.565	469.32	287.630	535.19
47.831	124.79	152.274	468.33	290.108	539.54
49.421	128.87	154.978	465.59	292.570	543.58
51.510	134.17	157.681	460.30	295.015	547.37
53.482	138.88	160.388	453.91	297.459	550.84
55.356	143.38	163.101	447.34	299.901	555.07
57.146	147.14	165.823	439.57	302.334	559.46
58.864	151.50	168.551	432.99	304.760	562.56
60.678	155.55	171.284	427.38	307.178	565.72
62.586	159.87	174.022	422.91	309.589	569.25
64.425	163.99	176.760	419.68	311.899	572.55
66.273	167.89	179.498	417.04	314.608	577.18
68.135	171.94	182.232	415.69	317.442	581.10
70.007	175.92	184.962	414.88	320.398	585.35
71.892	179.87	187.686	414.84	323.342	590.41
73.724	183.70	190.400	415.16	326.306	595.38
75.509	187.39	193.106	415.83	329.289	600.51
77.250	190.98	195.804	417.14	332.259	605.58
78.952	194.49	198.491	418.86	335.216	610.50
80.619	197.92	201.169	420.65	338.161	615.36
82.251	201.30	203.836	422.80	341.094	619.92
83.853	204.62	206.492	425.06	344.015	624.60
85.426	207.91	209.138	427.28	346.924	629.12
86.972	211.25	211.772	430.12	349.854	633.81
88.734	215.06	214.396	432.62	352.821	639.17
90.907	219.87	217.010	435.43	355.791	643.66

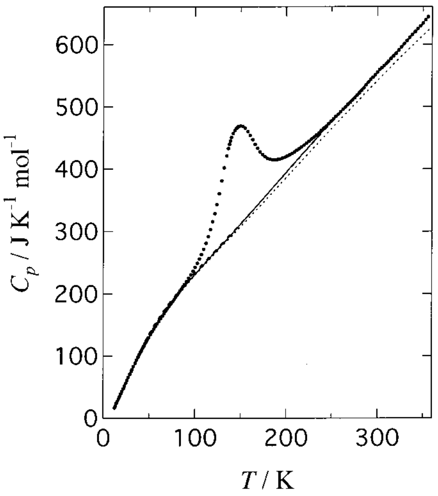

Figure 1. Plot of the molar heat capacity of [Fe(2-pic)$_3$]Cl$_2$·MeOH vs temperature. The dotted and dashed curves indicate the C_{lat}(LS) and the C_{lat}(HS), respectively. The solid curve shows the estimated normal heat capacity C_{lat} (see text).

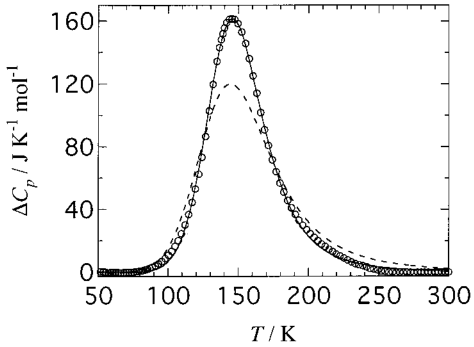

Figure 2. Excess heat capacity of [Fe(2-pic)$_3$]Cl$_2$·MeOH due to the spin crossover phenomenon. The broken curve indicates the theoretical values calculated by eq 11. The solid curve represents the least-squares fitting to the observed ΔC_p (see text).

The entropy gain is much larger than the value expected for the change in the spin manifold of a ferrous complex, R ln 5 (13.4 J K^{-1} mol^{-1}). From the previously reported crystal structure determinations,[14,19] it is clear that there is no disordering in the complex cation at the spin crossover transition. If there is no order–disorder transition also in the methanol solvate molecules, the remaining entropy gain of 46.1 J K^{-1} mol^{-1} can be considered to arise from the change in the internal vibrations. However, it should be remarked that this value is relatively large in comparison with those previously reported for the vibrational entropy change in the spin crossover phenomenon: 28.56 J K^{-1} mol^{-1} for [Fe(acpa)$_2$]PF$_6$,[5] 28.24 J K^{-1} mol^{-1} for [Fe(2-pic)$_3$]Cl$_2$·EtOH,[10] and 35.40 J K^{-1} mol^{-1} for [Fe(phen)$_2$(NCS)$_2$].[4] Since [Fe(2-pic)$_3$]Cl$_2$·MeOH and [Fe(2-pic)$_3$]Cl$_2$·EtOH consist of the same complex cation and Cl anions, and moreover, they have very similar crystal structures,[14] it is unclear why the entropy gains should be so different. Because the previous reports on the crystal structure determination of the title complex[14,18] have not stated whether the methanol solvate molecule is disordered or not, one cannot exclude the possibility that the excess entropy gain includes the contribution from the disordering of the methanol solvate molecules.

Although there have been reported several theoretical approaches to the spin crossover phenomena, such as elastic model,[19–22] Ising-like model,[23] and vibronic model,[24,25] we shall discuss the present results in terms of the domain model developed by Sorai and Seki[4] because our main interest is to elucidate the "cooperativity" of the present spin crossover

---

(18) Greenaway, A. M.; Sinn, E. *J. Am. Chem. Soc.* **1978**, *100*, 8080.

(19) Adler, P.; Wiehl, L.; Meissner, E.; Köhler, C. P.; Spiering, H.; Gütlich, P. *J. Phys. Chem. Solids* **1987**, *48*, 517.

(20) Willenbacher, N.; Spiering, H. *J. Phys. C: Solid State Phys.* **1988**, *21*, 1423.

(21) Spiering, H.; Willenbacher, N. *J. Phys.: Condens. Matter* **1989**, *1*, 10089.

(22) Spiering, H.; Meissner, E.; Köppen, H.; Müller, E. W.; Gütlich, P. *Chem. Phys.* **1994**, *68*, 65.

(23) Lemercier, G.; Bouseksou, A.; Seigneuric, S.; Varret, F.; Tuchagues, J.-P. *Chem. Phys. Lett.* **1994**, *226*, 289.

(24) Zimmerman, R.; König, E. *J. Phys. Chem. Solids* **1977**, *38*, 779.

(25) Kambara, T. *J. Chem. Phys.* **1979**, *70*, 4199.

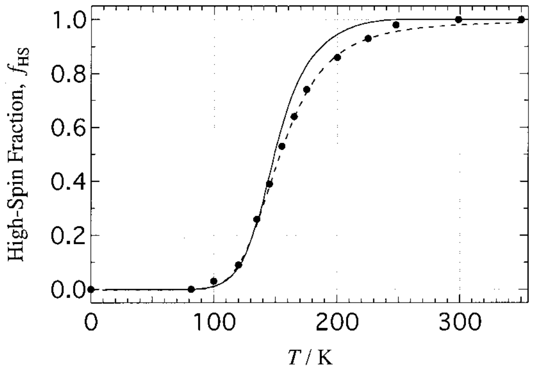

Figure 3. Temperature dependence of the HS fraction of $[Fe(2\text{-pic})_3]Cl_2 \cdot MeOH$.[15] The broken curve indicates the least-squares fit based on the domain model given by eq 4. The solid curve shows the high-spin fraction derived from the present calorimetric measurement (eq 7).

phenomenon. According to the domain model, the HS fraction can be written as

$$f_{HS} = \frac{1}{1 + \exp\left[\frac{n\Delta_{trs}H}{R}\left(\frac{1}{T} - \frac{1}{T_c}\right)\right]} \tag{4}$$

where $\Delta_{trs}H$ is the total enthalpy change due to the heat capacity anomaly and T_c is the critical temperature defined as the temperature at which both the LS and the HS fractions become 0.5. In the present calorimetric measurement, we have obtained the total enthalpy change $\Delta_{trs}H = 8.88$ kJ mol^{-1}. The number of molecules per domain n can be estimated by the least-squares fit of eq 4 to the experimental HS fraction. Figure 3 shows the least-squares fit of the temperature dependence of the high-spin fraction f_{HS} taken from the previous report.[15] In this fitting, the critical temperature was taken as $T_c = 153.2$ K. The obtained value $n = 1.12$ is very close to unity. In the case of $n = 1$, eq 4 is equivalent to the van't Hoff equation

$$\frac{d\ln K_{eq}}{dT} = \frac{\Delta_{trs}H}{RT^2} \tag{5}$$

where K_{eq} stands for the equilibrium constant given by

$$K_{eq} = \frac{f_{HS}}{f_{LS}} = \frac{f_{HS}}{1 - f_{HS}} \tag{6}$$

If this is the case, the temperature-induced spin crossover phenomenon completely obeys the Le Chatelier−Brown's law, in which the cooperative effect is absent just like in the liquid solution.

From the thermodynamic point of view, the HS fraction at a given temperature can be derived from the following equation

$$f_{HS} = \frac{\Delta H(T)}{\Delta_{trs}H} \tag{7}$$

where $\Delta H(T)$ means the enthalpy gain at a temperature T. The HS fraction obtained calorimetrically is shown in Figure 3 by the solid curve. The difference between the two sets of the f_{HS} is seen around ~200 K. The $f_{HS} - T$ curve derived from eq 7 is steeper than that derived from ^{57}Fe Mössbauer spectra. Some reasons can be considered for this deviation, such as (i) different recoilless fraction of ^{57}Fe nucleus between the HS isomer and the LS isomer, (ii) an overestimation of the lattice heat capacity, C_{lat}, especially for C_{lat}(HS), and (iii) different specimens used for the Mössbauer measurement and the present heat capacity measurement. The relative HS fraction f_{HS} was taken from the area fractions from the HS species assuming equal Lamb−Mössbauer factors for the HS and the LS isomers at a given temperature. If they are different, the area fraction does not agree with the actual isomer fraction. To circumvent this problem, it is better to use the f_{HS} derived from the effective magnetic moment by the following equation

$$\mu_{eff}^2 = f_{HS}\mu_{eff}(HS)^2 + (1 - f_{HS})\mu_{eff}(LS)^2 \tag{8}$$

Unfortunately, there are no available numerical magnetic data suitable for this calculation, although a plot of magnetic moments is presented in the previous publication.[18] However, almost equal recoilless fractions for both spin isomers have been found for some ferrous spin crossover complexes, such as $[Fe(bptn)_2(NCS)_2]$ (bptn = N,N'-bis(2-pyridylmethyl)-1,3-propanediamine),[26] $[Fe(2\text{-pic})_3]Cl_2 \cdot EtOH$,[27] and $Fe(trim)_2(PhCO_2)(ClO_4)$ (trim = 4′-(4-methylimidazole)-2′-(2″-methylimidazole)imidazole),[23] by comparing Mössbauer data and magnetic susceptibility data. Therefore, it is very likely that the possibility of (i) is low in the present complex. We shall consider next the possibility of (ii). When we determine the lattice heat capacity of the HS state C_{lat}(HS), we used the C_p data in the ranges of $T > 250$ K and the 12−23 K range as if they belonged to the HS state. At very low temperatures, this assumption would scarcely affect the results, because the difference between C_{lat}(LS) and C_{lat}(HS) is very small. In the higher temperature region, however, if the HS fraction obeys eq 4, the thermal anomaly never terminates at a finite temperature, implying that the C_p values do not coincide with the lattice heat capacity C_{lat}(HS) in the 250−355 K temperature range. It should be remarked here that the calorimetric definition given by eq 7 is valid for the first-order phase transition occurring isothermoally. As a matter of fact, purity determination by the fractional melting method for organic substances is made on the basis of the fraction estimated from eq 7. This assumes that the enthalpy change between crystal and liquid is independent of the fraction melted (in the present case, the HS fraction f_{HS}). However, when a change occurs over a wide temperature region as in the case of the present gradual-type spin crossover, it is very likely that the enthalpy increment, analogous to the partial molar enthalpy encountered in binary component systems, would be a function of how many of its neighbors are high spin or low spin. One of the plausible reasons for the small discrepancy of the HS-fraction determined calorimetrically from the observed temperature dependence (Figure 3) may be a disregard of such a weak cooperative coupling between the neighbors. Although both (ii) and (iii) cannot be excluded at the present stage, the theoretical and experimental data seem to agree rather well with each other as far as we take into account the fact that the data have been obtained for different samples on the basis of different methods.

The excess heat capacity at a given temperature can also be evaluated thermodynamically by the differential of the enthalpy as follows

$$\Delta C_p(T) = \frac{d\Delta H(T)}{dT} \tag{9}$$

where

$$\Delta H(T) = f_{HS} \times \Delta_{trs}H \tag{10}$$

Equations 4, 9, and 10 give the following equation:

$$\Delta C_{\mathrm{p}}(T) = \frac{n(\Delta_{\mathrm{trs}}H)^2}{RT^2} \frac{\exp\left[\dfrac{n(\Delta_{\mathrm{trs}}H)}{R}\left(\dfrac{1}{T} - \dfrac{1}{T_{\mathrm{c}}}\right)\right]}{\left\{1 + \exp\left[\dfrac{n(\Delta_{\mathrm{trs}}H)}{R}\left(\dfrac{1}{T} - \dfrac{1}{T_{\mathrm{c}}}\right)\right]\right\}^2} \qquad (11)$$

To evaluate the theoretical ΔC_{p} curve, we adopted $n = 1.12$, $\Delta_{\mathrm{trs}}H = 8.88$ kJ mol^{-1}, and $T_{\mathrm{c}} = 153.2$ K. The resultant curve is shown in Figure 2 by the broken curve. The quantitative agreement seems to be not so good, but eq 11 rather well reproduces the asymmetric ΔC_{p} curve although the n and T_{c} were determined independently of the present heat capacity measurement. Here again, a plausible reason for the small discrepancy seen in ΔC_{p} between the domain model (the broken curve in Figure 2) and the observed temperature dependence would be that the cooperative coupling interactions between neighboring domains have been ignored in the present domain model.

On the other hand, if eq 11 is independently fitted to the experimental ΔC_{p} with two adjustable parameters n and T_{c} by the least-squares fit, one obtains $n = 1.50$ and $T_{\mathrm{c}} = 150.8$ K. The values of these two parameters are very close to $n = 1.12$ and $T_{\mathrm{c}} = 153.5$ K determined on the basis of the Mössbauer measurement.[15] The solid curve shown in Figure 2 indicates this least-squares fit. Although there exists a slight discrepancy between the two curves evaluated from different methods, they provide us with the same conclusion that the number of complexes per domain is substantially unity, and thus, the cooperativity in the present complex is extremely weak or absent.

Concluding Remarks. The present heat capacity measurements have confirmed that the spin crossover phenomenon in [Fe(2-pic)$_3$]Cl$_2$·MeOH is essentially noncooperative and that the two types of molecules with different spin states are in an equilibrium state, i.e., a solid-solution is formed by the LS and the HS species. Such a solid-solution state is consistent with previously reported multi-temperature single-crystal X-ray structural determination, where two fractional types of molecules have been taken into account at a given lattice site.[14] Kulshreshtha et al.[28] have also observed no well-defined peak in the DSC thermograms of [Fe(bts)$_2$(NCS)$_2$] (bts = 2,2′-bi-5-methyl-2-thiazoline), which shows a gradual type of spin crossover phenomenon ($T_{\mathrm{c}} \approx 219.5$ K), and concluded that the two types of molecules with different spin states exist as a solid-solution in the same lattice. They have suggested that the enthalpy change associated with the spin transition of [Fe(bts)$_2$(NCS)$_2$] is rather small. However, for the present complex the $\Delta_{\mathrm{trs}}H$ and $\Delta_{\mathrm{trs}}S$ values are as large as those for the abrupt transition type complexes, for example, $\Delta_{\mathrm{trs}}H = 8.60$ kJ mol^{-1} and $\Delta_{\mathrm{trs}}S = 48.78$ J K^{-1} mol^{-1} for [Fe(phen)$_2$(NCS)$_2$].[4] This fact means that the noncooperative spin crossover phenomenon also involves enthalpy and entropy changes comparable with those of the cooperative spin crossover phenomenon, although there still remains a possibility of the entropy contribution from order−disorder of the methanol solvate molecules. The standard thermodynamic quantities of [Fe(2-pic)$_3$]Cl$_2$·MeOH have been determined and are tabulated in Table 2.

Table 2. Standard Thermodynamic Functions for [Fe(2-pic)$_3$]Cl$_2$·MeOH at Rounded Temperatures[a]

T (K)	$C^{\circ}_{\mathrm{p,m}}$ (J K^{-1} mol^{-1})	$S^{\circ}_{\mathrm{m}}(T)$ (J K^{-1} mol^{-1})	$\{H^{\circ}_{\mathrm{m}}(T) - H^{\circ}_{\mathrm{m}}(0)\}/T$ (J K^{-1} mol^{-1})	$\{G^{\circ}_{\mathrm{m}}(T) - H^{\circ}_{\mathrm{m}}(0)\}/T$ (J K^{-1} mol^{-1})
5	(4.81)	(2.935)	(1.949)	(0.986)
10	(11.82)	(8.144)	(4.927)	(3.218)
15	25.37	15.222	9.258	5.963
20	41.10	24.663	15.238	9.425
30	73.51	47.516	29.312	18.204
40	103.58	72.864	44.198	28.666
50	130.34	98.923	58.829	40.094
60	154.03	124.813	72.743	52.070
70	175.90	150.220	85.944	64.275
80	196.64	175.070	98.482	76.587
90	217.86	199.439	110.555	88.883
100	241.83	223.595	122.457	101.138
120	319.04	273.609	147.956	125.653
140	451.30	332.941	182.056	150.885
160	454.83	394.859	217.276	177.583
180	416.79	445.813	241.156	204.658
200	419.87	489.662	258.653	231.009
220	438.64	530.493	274.104	256.389
240	463.98	569.709	288.829	280.880
260	492.16	607.936	303.369	304.567
280	521.97	645.502	317.921	327.582
300	555.25	682.728	332.710	350.018
320	584.78	719.513	347.550	371.963
340	618.22	755.978	362.495	393.484
298.15	552.04	679.304	331.338	347.966

[a] The values in parenthses were estimated by the effective frequency distribution method.[17]

Acknowledgment. This work was partially supported by a Grant-in-Aid for Scientific Research on the Priority Areas of "metal-assembled complexes" (Area No. 401/12023229) from the Ministry of Education, Science, Sports and Culture, Japan.

IC010073Z

---

(26) Yu, Z.; Schmitt, G.; Böres, N.; Spiering, H.; Gütlich, P. *J. Phys.: Condens. Matter* **1995**, *7*, 777.

(27) Köhler, C. P.; Jakobi, R.; Meissner, E.; Spiering, H.; Gütlich, P. *J. Phys. Chem. Solids* **1990**, *51*, 239.

(28) Kulshreshtha, S. K.; Iyer, R. M.; König, E.; Ritter, G. *Chem. Phys. Lett.* **1984**, *110*, 201.